PHILOSOPHICAL TRANSACTIONS A

rsta.royalsocietypublishing.org

Review

Cite this article: Adamatzky A. 2015 Slime mould processors, logic gates and sensors. *Phil. Trans. R. Soc. A* **373**: 20140216. http://dx.doi.org/10.1098/rsta.2014.0216

Accepted: 21 April 2015

One contribution of 13 to a Theo Murphy meeting issue 'Heterotic computing: exploiting hybrid computational devices'.

Subject Areas:
hybrid computing, theory of computing

Keywords:
slime mould, morphological computing, logic gates, sensors

Author for correspondence:
A. Adamatzky
e-mail: andrew.adamatzky@uwe.ac.uk

Downloaded from https://royalsocietypublishing.org/ on 28 November 2024

Slime mould processors, logic gates and sensors

A. Adamatzky

Unconventional Computing Centre, University of the West of England, Bristol, UK

A heterotic, or hybrid, computation implies that two or more substrates of different physical nature are merged into a single device with indistinguishable parts. These hybrid devices then undertake coherent acts on programmable and sensible processing of information. We study the potential of heterotic computers using slime mould acting under the guidance of chemical, mechanical and optical stimuli. Plasmodium of acellular slime mould *Physarum polycephalum* is a gigantic single cell visible to the unaided eye. The cell shows a rich spectrum of behavioural morphological patterns in response to changing environmental conditions. Given data represented by chemical or physical stimuli, we can employ and modify the behaviour of the slime mould to make it solve a range of computing and sensing tasks. We overview results of laboratory experimental studies on prototyping of the slime mould morphological processors for approximation of Voronoi diagrams, planar shapes and solving mazes, and discuss logic gates implemented via collision of active growing zones and tactile responses of *P. polycephalum*. We also overview a range of electronic components—memristor, chemical, tactile and colour sensors—made of the slime mould.

1. Introduction

Slime mould *Physarum polycephalum* belongs to the species of order Physarales, subclass Myxogastromycetidae, class Myxomycetes, division Myxostelida. It is commonly known as a true, acellular or multi-headed slime mould. *Physarum polycephalum* has a rich life cycle [1]: fruit body, spore, single-cell amoeba, syncytium and plasmodium. Plasmodium is a 'vegetative' phase, a single cell with a myriad of diploid nuclei. The plasmodium is visible to the unaided eye: its size ranges from a few centimetres to a few metres. The plasmodium looks like an amorphous yellowish mass with networks of protoplasmic tubes. It behaves and

THE ROYAL SOCIETY PUBLISHING

© 2015 The Author(s) Published by the Royal Society. All rights reserved.

Downloaded from https://royalsocietypublishing.org/ on 28 November 2024

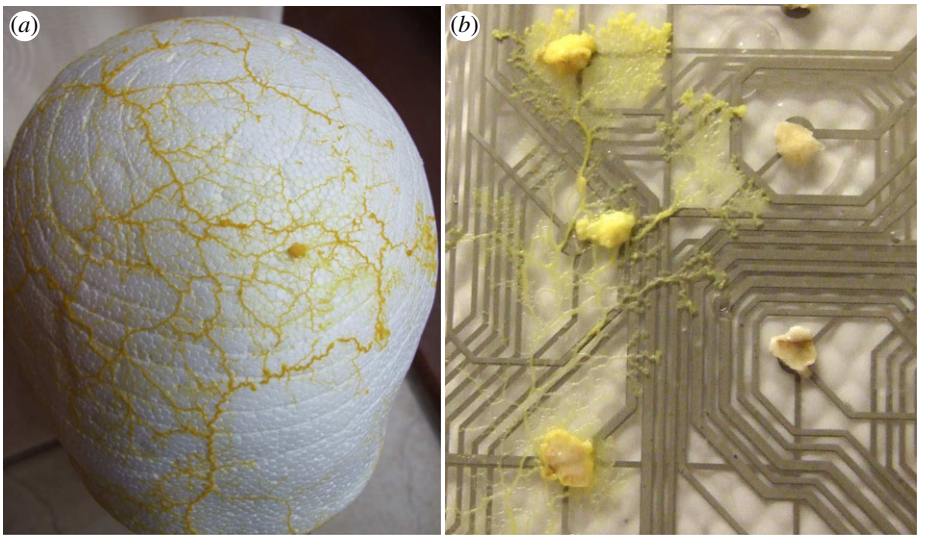

Figure 1. Plasmodium of *P. polycephalum* propagating on a polyurethane model of human head (*a*) and colonizing oat flakes on a plastic sheet with a conductive circuit (*b*). (Online version in colour.)

moves as a giant amoeba. It feeds on bacteria, spores and other microbial creatures and micro-particles [1]. Given enough air humidity, the slime mould can inhabit literally any substrate (figure 1). During its foraging behaviour, the plasmodium spans scattered sources of nutrients with a network of protoplasmic tubes.

The plasmodium optimizes its protoplasmic network that covers all sources of nutrients and guarantees robust and rapid distribution of nutrients in the plasmodium's body. The plasmodium's foraging behaviour can be interpreted as a computation [2–4]: data are represented by a spatial distribution of attractants and repellents, and results are represented by the structure of the protoplasmic network. The plasmodium can solve computational problems with natural parallelism, e.g. related to the shortest path and hierarchies of planar proximity graphs, execution of logical computing schemes and natural implementation of spatial logic and process algebra [5].

We developed a concept and designed a series of experimental laboratory prototypes of computing devices—Physarum machines [5]—based on *P. polycephalum*. A Physarum machine is a programmable amorphous biological computing device experimentally implemented in plasmodium of *P. polycephalum*. A Physarum machine is programmed by configurations of repelling and attracting gradients. See the detailed analysis of Physarum machines in [5]. The mechanics of Physarum machines is based on the following unique features of *P. polycephalum*. Physarum is a reaction–diffusion excitable medium encapsulated in an elastic growing membrane (excitation is triggered by chemical, physical and mechanical stimuli). Physarum may be regarded as a living micro-manipulation and micro-fluidic transport device. Physarum represents the results of a computation by the configuration of its body: the topology of the Physarum network is influenced by its environment, distribution and gradients of chemoattractants and chemorepellents. Physarum is sensitive to illumination, therefore allowing for parallel input of information.

We overview the computing and sensing potential of Physarum in a series of experimental laboratory studies and demonstrate that the plasmodium of *P. polycephalum* can be used as a computational geometry and optimization processor (§2) and as Boolean logic circuits (§3), memristors (§4) and chemical, mechanical and colour sensors (§5).

2. Morphological processors

Physarum represents the results of computation by changing the morphology of its body. In three examples, we show what types of data encoding can be used to program behaviour of

Downloaded from https://royalsocietypublishing.org/ on 28 November 2024

Physarum and produce deterministic results. In the first example, a Voronoi diagram (§2a), data are represented by pieces of the slime mould inoculated on a planar substrate. The second example, planar shapes (§2b), uses a combination of attractants and repellents as input data. Morphological computation assisted by diffusion of attractants and competing between active growing zones of the plasmodium is demonstrated in the third example, solving mazes (§2c).

(a) Voronoi diagram

Let **P** be a non-empty finite set of planar points. A planar Voronoi diagram of the set **P** is a partition of the plane into such regions that, for any element of **P**, a region corresponding to a unique point p contains all those points of the plane which are closer to p than to any other node of **P**. A unique region $\mathrm{vor}(p) = \{z \in \mathbf{R}^2 : d(p,z) < d(m,z) \forall\ m \in \mathbf{P}, m \neq p\}$ assigned to the point p is called a Voronoi cell of the point p. The boundary of the Voronoi cell of the point p is built of segments of bisectors separating pairs of geographically closest points of the given planar set **P**. A union of all boundaries of the Voronoi cells determines the *planar Voronoi diagram*: $\mathrm{VD}(\mathbf{P}) = \cup_{p \in \mathbf{P}} \partial \mathrm{vor}(p)$ [6]. The basic concept of constructing Voronoi diagrams with reaction–diffusion systems is based on an intuitive technique for detecting the bisector points separating two given points of the set **P**. If we drop reagents at the two data points, the diffusive waves or phase waves, if the computing substrate is active, travel outwards from the drops. The waves travel the same distance from the sites of origin before they meet one another. The points where the waves meet are the bisector points [7].

The plasmodium growing on a nutrient substrate from a single site of inoculation expands circularly as a typical diffusive or excitation wave. When two plasmodium waves encounter each other, they stop propagating. To approximate a Voronoi diagram with Physarum, we physically map a configuration of planar data points by inoculating plasmodia on a substrate (figure 2*a*). Plasmodium waves propagate circularly from each datum point (figure 2*b*,*c*) and stop when they collide with each other (figure 2*d*). Thus, the plasmodium waves approximate a Voronoi diagram, whose edges are the substrate's loci not occupied by plasmodia (figures 2*d* and 3*a*).

Plasmodium growing on a nutrient-rich substrate approximates a planar Voronoi diagram.

The plasmodia do not stop their propagation forever. In 10–15 h, they resume their activity, protoplasmic tubes percolate between temporarily 'frozen' wavefronts and the plasmodia originating from different data points merge into a single organism (figure 3*b*).

(b) α-shapes

The convex hull of a finite set **P** of planar points is the smallest convex polygon that contains all points of **P** (figure 4*a*). The α-hull of **P**, $\alpha > 0$, is an intersection of the complements of all closed discs of radius $1/\alpha$ that include no points of **P** [8,9]. The α-shapes converge to the convex hull as $\alpha \to \infty$. With a decrease of α, the shapes may shrink, develop holes and become disconnected; the shapes collapse to **P** when $\alpha \to 0$. A concave hull is a non-convex polygon representing the area occupied by **P**. A concave hull is a connected α-shape without holes (figure 4*b*). We want slime mould to solve the following problem. Given planar set **P** represented by physical objects, the plasmodium of *P. polycephalum* must represent the concave hull of **P** by its largest protoplasmic tube.

The first algorithm of convex hull construction [10] was based on cognitive tactic techniques we use in our everyday life. We select a starting point which is an extremal point of **P**. We pull a rope (anti-)clockwise to another extremal point. We continue until the set **P** is wrapped completely. The computation stops when we reach the starting point. Let us represent data points of **P** by sources of attractants only, e.g. by oat flakes (figure 5*a*). We place a piece of plasmodium at some distance away from the set of points (figure 5*a*). The plasmodium propagates towards set **P**, colonizes oat flakes (figure 5*a*,*b*) and spans them with a network of protoplasmic tubes (figure 5*c*). No hull is constructed. When all data points **P** are colonized and spanned by the protoplasmic network, the

Downloaded from https://royalsocietypublishing.org/ on 28 November 2024

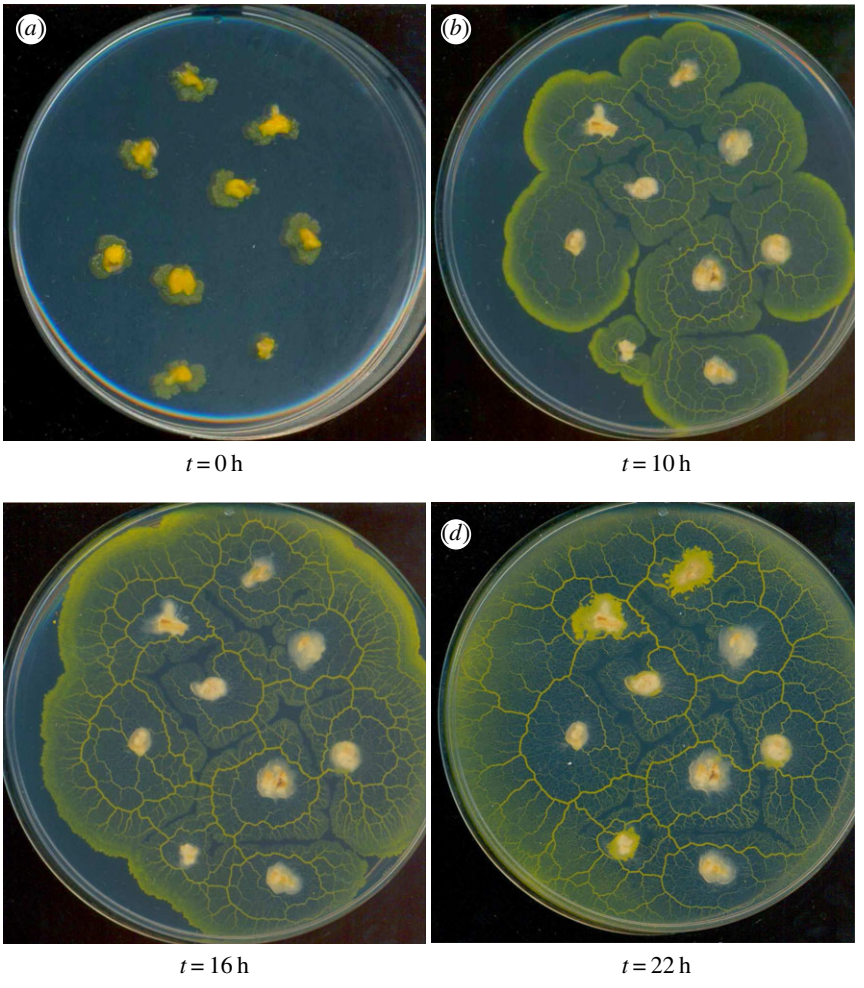

Figure 2. Approximation of a Voronoi diagram by Physarum on 2% corn meal agar (Fluka): (*a*) sites of plasmodium inoculation represent planar data points to be sub-divided by the edges of the Voronoi diagram, (*b*, *c*) propagation of growing plasmodia, (*d*) bisectors of the Voronoi diagram are represented by loci of substrate not occupied by plasmodium. (Online version in colour.)

plasmodium ventures to explore the space around **P** and thus loses all chances of constructing any shapes of **P** [11].

Physarum polycephalum does not compute the concave or convex hulls of a set represented by attracting sources.

Using repellents only, for example as a set of obstacles between attractants and the inoculation site, will do no good because plasmodium will just pass around the repellents (see details in [5]), controlling Physarum with salt. The only solution would be to employ attractants to 'pull' plasmodium towards planar set **P** and to use repellents to prevent plasmodium from spanning the points of **P**. The strength of the repellents should be proportional to α and thus will determine the exact shape of the constructed hull. This corresponds to the definition [8] that α-hull of **P** is the intersection of all closed discs with radius $1/\alpha$ that contain all the points of **P**.

The plasmodium of *P. polycephalum* approximates the connected α-hull without holes of a finite planar set, where points are represented by sources of long-distance attractants and short-distance repellents [11].

When presented with a half-pill of the Kalms Night sleep tablets (G. R. Lane Health Products Ltd, Gloucester GL2 0GR, UK; the main ingredients are valerian and hops extracts) [12], the

Downloaded from https://royalsocietypublishing.org/ on 28 November 2024

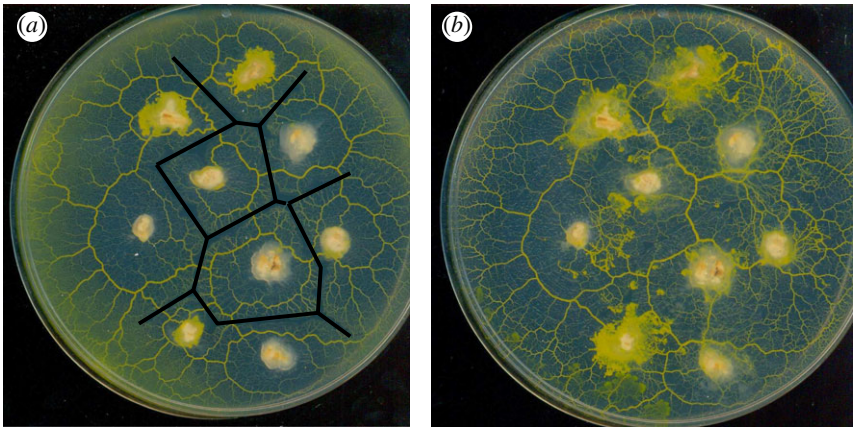

Figure 3. A Voronoi diagram approximated by Physarum (*a*), constructed during the first 22 h after inoculation. Bisectors of the diagram are represented by loci of substrate not colonized by plasmodium; they are indicated by solid lines. Plasmodia occupy the empty loci of the substrate in the next 12 h (*b*). (Online version in colour.)

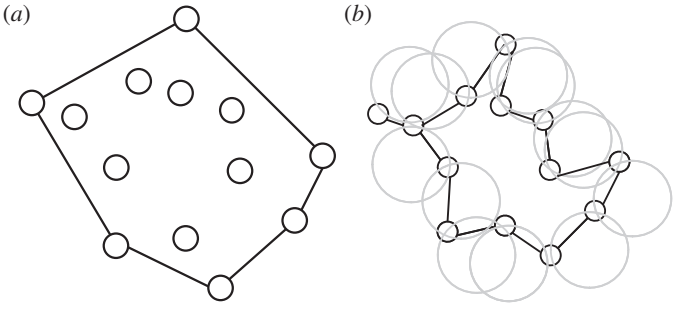

Figure 4. Planar hulls. (*a*) Example of a convex hull. (*b*) Example of a concave hull. Points of set **P** are shown as empty discs.

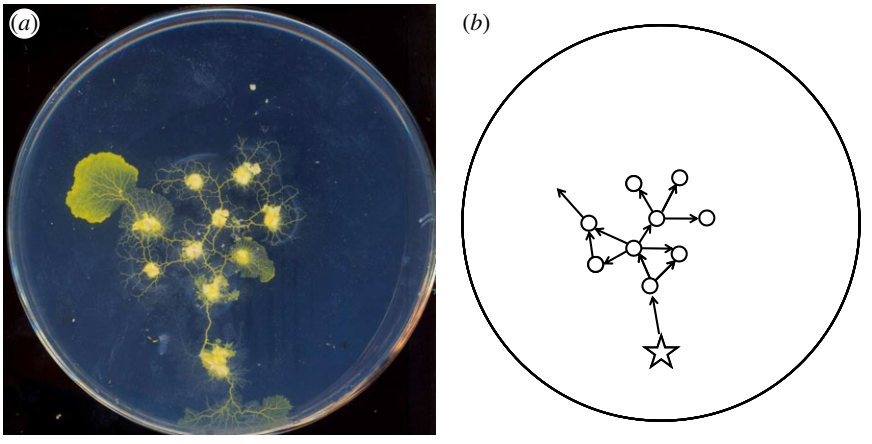

Figure 5. Slime mould spans oat flakes. (*a*) Spanning oat flakes, representing **P**, by a network of protoplasmic tubes: scanned image. (*b*) Scheme of the plasmodium propagation, circles are points, or oat flakes, of **P** and star marks the site of inoculation; arrows are protoplasmic tubes. (Online version in colour.)

Downloaded from https://royalsocietypublishing.org/ on 28 November 2024

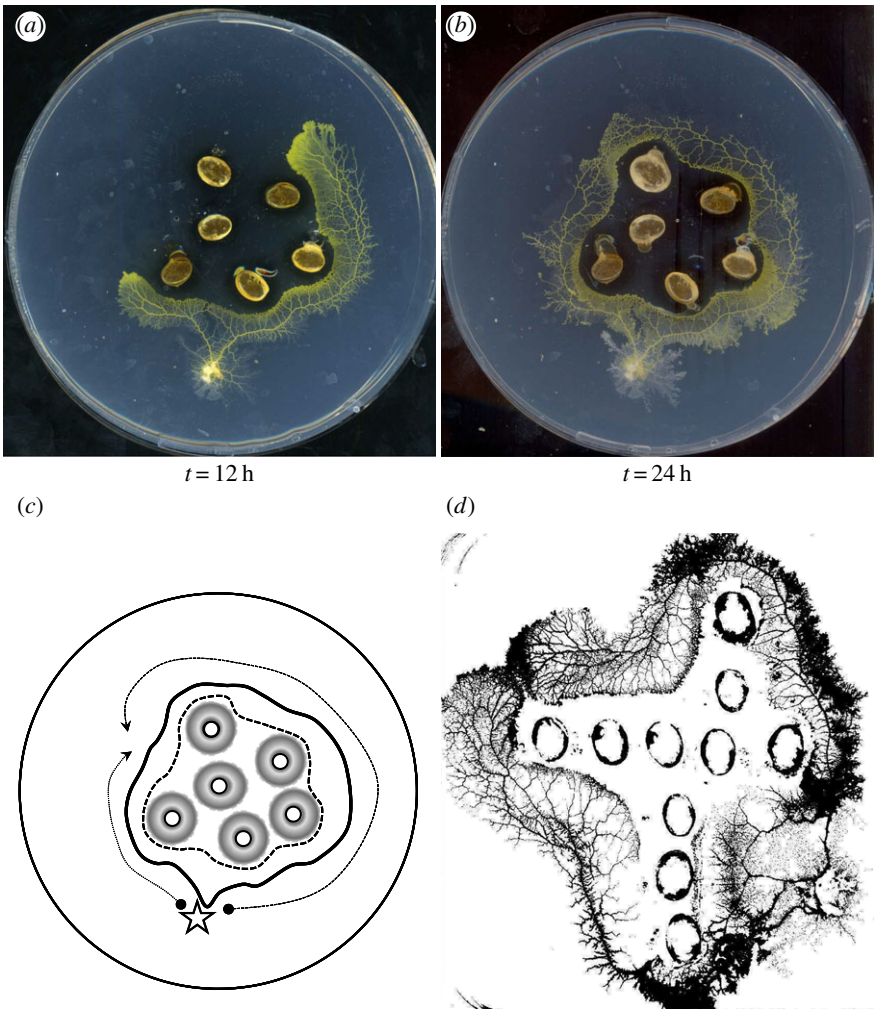

Figure 6. Computation of concave hulls of point set **P**. (*a*, *b*) Photographs 12 h (*a*) and 24 h (*b*) after plasmodium's inoculation. (*c*) Scheme of the plasmodium interaction with **P**: points of **P** are shown as circles; diffusing repellents, visible as black halos surrounding pills in figure 6*a*,*c*, are shown by grey gradients; the feeding boundary of the protoplasm is marked by the dotted line; the major protoplasmic tube, which approximates CH(**P**), is shown by the solid line. (*d*) Binarized image of plasmodium approximating the concave hull of **P**. (Online version in colour.)

plasmodium propagates towards the pill and forms, with its protoplasmic tubes, a circular enclosure around the pill. Such a unique behaviour of plasmodium in the presence of Kalms Night sleep tablets indicates that a plasmodium could implement Jarvis's gift-wrapping algorithm [10], adapted to concave hulls, if points of **P** are represented by the pills.

We tested the feasibility of the idea in 25 experiments [11]. All experiments were successful. In each experiment, we arranged four to eight half-pills (they represent given planar set **P**) in a random fashion near the centre of a Petri dish and inoculated an oat flake colonized by plasmodium 2–4 cm away from the set **P**. A typical experiment is illustrated in figure 6. Twelve hours after inoculation, the plasmodium propagates towards set **P** and starts enveloping the set with its body and network of protoplasmic tubes (figure 6). The plasmodium completes an approximation of the shape by entirely enveloping **P** in the next 12 h (figure 6). The plasmodium does not propagate inside the configuration of pills (figure 6). The scheme of the concave hull construction is shown in figure 6*c*. The configuration of **P** in figure 6*a*–*d* favours the approximation of a convex hull. If the spatial configuration of the points curves inwards, then a concave hull is approximated (figure 6*d*).

Downloaded from https://royalsocietypublishing.org/ on 28 November 2024

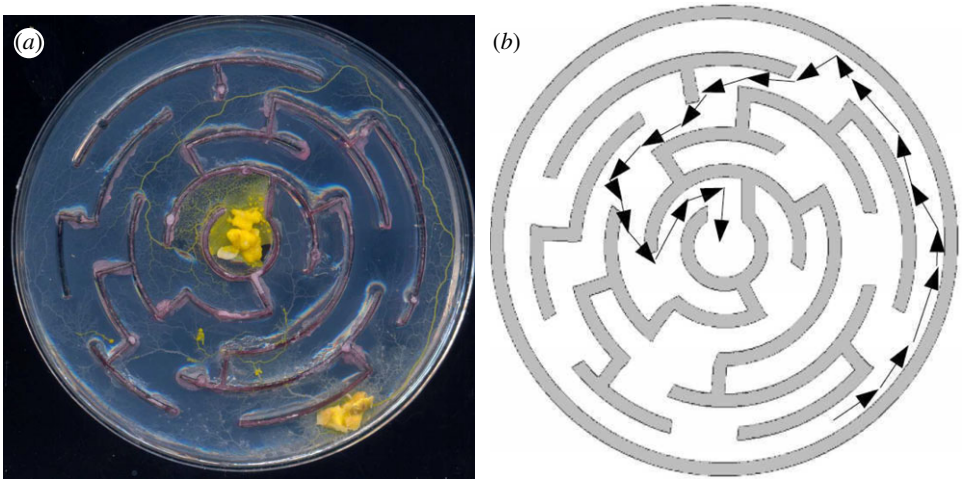

Figure 7. Experimental maze-solving with plasmodium of Physarum. The plasmodium is inoculated in a peripheral channel, in the east part of the maze, and a virgin oat flake is placed in the central chamber. (*a*) Scanned image of the experimental maze; protoplasmic tubes are yellow (light grey); (*b*) scheme of the plasmodium propagation; arrows symbolize the velocity vectors of the propagating active zone. (Online version in colour.)

(c) Maze

When solving the maze problem, Shannon's electromagnetic mouse Theseus explored all possible passages, while marking visited parts, until the exit or a central chamber was found [13]. Things did not change substantially with physical computing devices that approximate the shortest path or solve a maze. For example, in a gas-discharge maze-solver [14], an electric field, generated between the source and destination electrodes, explores a maze in parallel. The field is stronger along the shortest path between the source and destination electrodes; therefore, channels of the shortest path glow with high intensity. A slime mould maze-solver reported in [3] requires Physarum to be placed in virtually every site of the maze. Initially, the plasmodium develops a network of protoplasmic tubes spanning all channels of the maze, thus representing all possible solutions. Then oat flakes are placed in the source and destination sites and the plasmodium enhances the tube connecting the source and destination along the shortest path. Selection of the shortest protoplasmic tube is implemented via interaction of propagating bio-chemical, electric potential and contractile waves in the plasmodium's body. The longest and cul-de-sac branches are abandoned. Thus, we can call the prototype [3] a 'pruning plasmodium'. The largest protoplasmic tube (more precisely, its walls), which represents the shortest path, remains visible even when the plasmodium ceases functioning. Therefore, we can consider the slime mould maze-solver as having non-volatile memory (analogous to precipitating reaction–diffusion chemical processors).

In laboratory prototypes of a mobile droplet [15] and hot ice computer [16], the computation of the shortest path in a maze is separated into two stages: computation of the many-sources-one-destination set of paths and extraction of a shortest path from the set of paths. The many-sources-one-destination paths are computed by spreading acidity in [15] and propagating a crystallization pattern in [16]. The shortest path is selected and traced by a droplet travelling along the pH gradient [15] or a virtual robot traversing the crystallization pattern [16]. We apply the two-stage computation in the design of a slime mould maze-solver which navigates a maze in one go, without exploring all possible options because the options are 'explored' by chemoattractants emitted by the destination oat flake.

In laboratory experiments, we used plastic mazes 70 mm in diameter with 4 mm wide and 3 mm deep channels (figure 7*a*). We filled the channels with 2% agar gel (Select agar; Sigma

Downloaded from https://royalsocietypublishing.org/ on 28 November 2024

Aldrich) as a non-nutrient substrate. We smeared the top of the channel walls with Vaseline (Unilever, Leatherhead, UK) to deter the plasmodium from making 'illegal' shortcuts over the walls separating the channels. A rolled oat was placed in the central chamber of the maze and an oat flake colonized by plasmodium of Physarum was placed in the most peripheral channel of the maze. Typically, it takes Physarum 1–3 days to propagate towards the central chamber of the maze.

A typical experiment is illustrated in figure 7. We placed an oat flake in the central chamber and inoculated the plasmodium of Physarum in a peripheral channel. The plasmodium started exploring its vicinity and at first generated two active zones, propagating clock- and anti-clockwise. By the time the diffusing chemoattractants reached the distant channels, one of the active zones had already became dominant and suppressed another the active zone. In the example shown in figure 7, the active zone travelling anti-clockwise dominated and 'extinguished' the active zone propagating clockwise. The dominating active zone then followed the gradient of chemoattractants inside the maze, navigated along the intersections of the maze's channels and solved the maze by entering its central chamber.

3. Logic gates

Computing with the slime mould could be implemented in many different ways, determined by what functional features of Physarum are interpreted as outputs of its processing. Our first example, ballistic gates (§3a), shows how to realize logic gates using interactions between active growing zones of the slime mould. In our second example, microfluidic gates (§3b), we use changes in cytoplasmic flow in response to tactile stimulation.

(a) Ballistic gates

Given a cross-junction of agar channels, cut from 2–3 mm thick agar plate, and plasmodium inoculated in one of the channels, the plasmodium propagates straight through the junction [17]; the speed of propagation may increase if sources of chemoattractants are present. An active zone, or a growing tip, of plasmodium propagates in the initially chosen direction, as if it has some kind of inertia. Based on this phenomenon, we designed two Boolean gates with two inputs and two outputs (figure 8*a*,*b*). Input variables are x and y and outputs are p and q. The presence of a plasmodium in a given channel indicates TRUTH and its absence indicates FALSE. Each gate implements a transformation from $\langle x, y\rangle \rightarrow \langle p, q\rangle$. Experimental examples of the transformations are shown in figure 8.

The plasmodium of *P. polycephalum* implements a two-input, two-output Boolean gate P_1: $\langle x, y\rangle \rightarrow \langle xy, x + y\rangle$.

The plasmodium inoculated in input y of P_1 propagates along the channel yq and appears in the output q (figure 8*c*). The plasmodium inoculated in input x of P_1 propagates until the junction of x and y, 'collides' with the impassable edge of channel yq and appears in output q (figure 8*d*). When plasmodia are inoculated in both inputs x and y of P_1, they collide with each other and the plasmodium that originated in x continues along the route xp. Thus, the plasmodia appear in both outputs p and q (figure 8*e*).

The plasmodium of *P. polycephalum* implements a two-input, two-output gate P_2: $\langle x, y\rangle \rightarrow \langle x, \bar{x}y\rangle$.

If input x is empty, the plasmodium placed in input y of P_2 propagates directly towards output p (figure 8*f*). The plasmodium inoculated in input x of P_2 (when the input y is empty) travels directly towards output q (figure 8*g*). Thus, transformations $\langle 0, 1\rangle \rightarrow \langle 1, 0\rangle$ and $\langle 1, 0\rangle \rightarrow \langle 0, 1\rangle$ are implemented. The gate's structure is asymmetric, i.e. the x-channel is shorter than the y-channel. Therefore, the plasmodium placed in the input x of P_2 usually passes the junction by the time the plasmodium originated in input y arrives at the junction (figure 8*h*). The y-plasmodium merges with the x-plasmodium and they both propagate towards the output q (figure 8*i*). Extension of the gel substrate after output q usually facilitates implementation of the transformation $\langle 1, 1\rangle \rightarrow \langle 0, 1\rangle$.

Downloaded from https://royalsocietypublishing.org/ on 28 November 2024

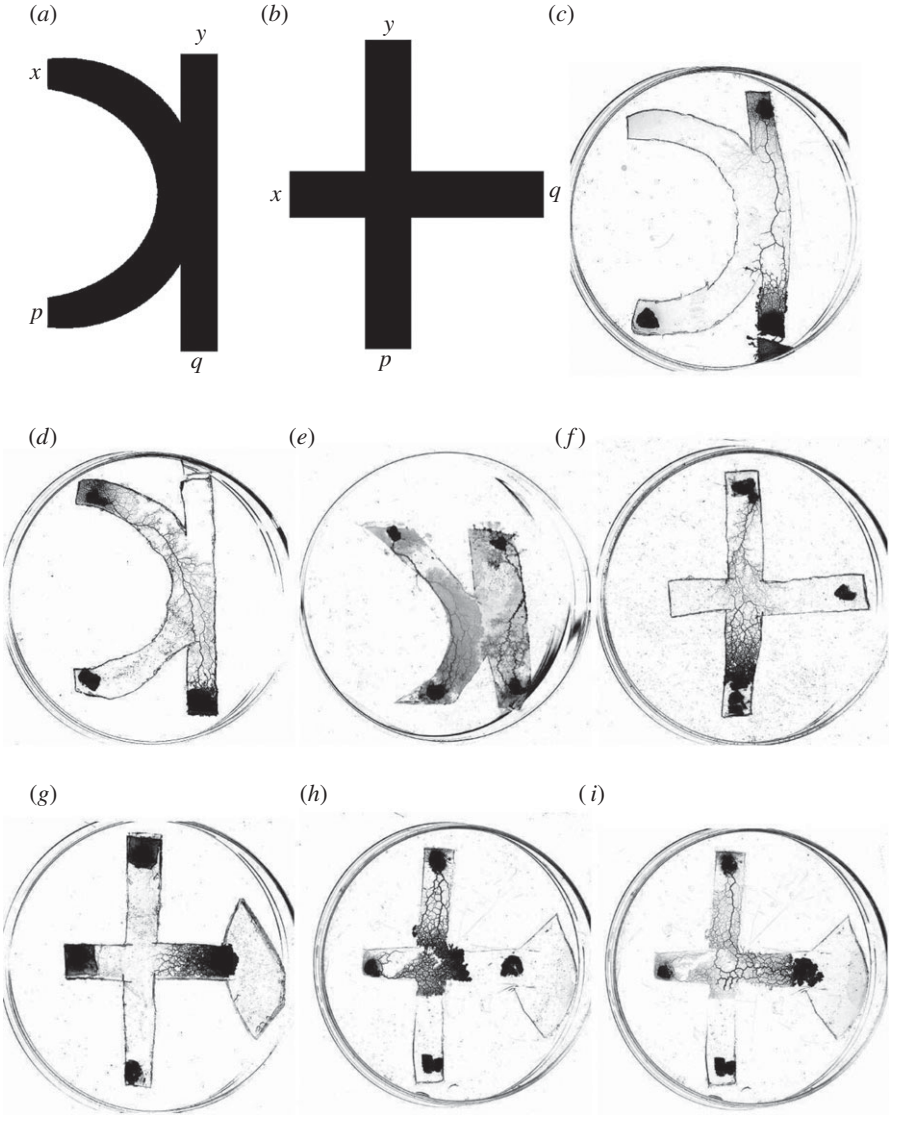

Figure 8. Physarum logic gates. (*a*, *b*) Geometrical structure of Physarum gates P_1 (*a*) and P_2 (*b*): x and y are inputs, p and q are outputs. (*c–e*) Experimental examples of transformation $\langle x, y\rangle \to \langle p, q\rangle$ implemented by Physarum gate P_1. (*c*) $\langle 0, 1\rangle \to \langle 0, 1\rangle$. (*d*) $\langle 1, 0\rangle \to \langle 0, 1\rangle$. (*e*) $\langle 1, 1\rangle \to \langle 1, 1\rangle$. (*f–i*) Experimental examples of transformation $\langle x, y\rangle \to \langle p, q\rangle$ implemented by Physarum gate P_2. (*f*) $\langle 0, 1\rangle \to \langle 1, 0\rangle$. (*g*) $\langle 1, 0\rangle \to \langle 0, 1\rangle$. (*h*, *i*) Two snapshots (taken with an 11 h interval) of transformation $\langle 1, 1\rangle \to \langle 0, 1\rangle$.

A one-bit half-adder is a logical circuit which takes two inputs, x and y, and produces two outputs: sum $\bar{x}y + x\bar{y}$ and carry xy. To construct a one-bit half-adder with Physarum gates, we need two copies of gate P_1 and two copies of gate P_2. Cascading the gates into the adder is shown in figure 9*a*. Signals x and y are inputted in the P_2 gates. Outputs of the P_2 gates are connected to inputs of the P_1 gates. We did not manage to realize a one-bit half-adder in experiments with living plasmodium because the plasmodium behaved differently in the assembly of the gates than in isolated gates. Therefore, we simulated the adder using the Oregonator model; see details in [17]. To simulate inputs $x = 0$ and $y = 1$, we initiated the plasmodium's active zones near the entrances to the channels, marked y and with an arrow in figure 9*a*. The active zones propagated along their channels (figure 9*b*).

Downloaded from https://royalsocietypublishing.org/ on 28 November 2024

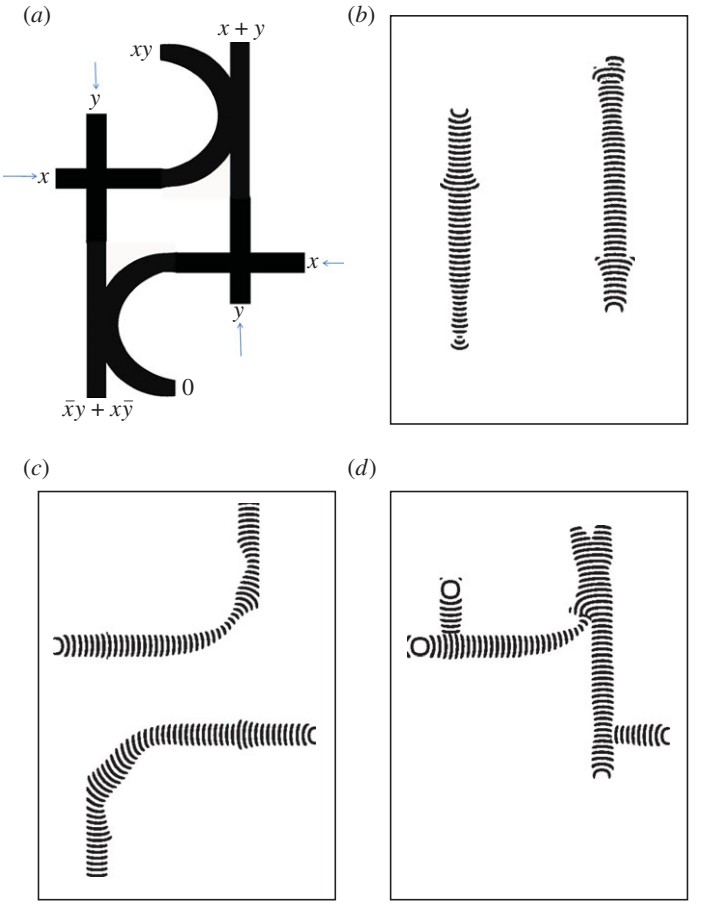

Figure 9. Simulation of a Physarum one-bit half-adder. (*a*) Scheme of a one-bit half-adder made of gates P_1 and P_2. Inputs are indicated by arrows. Outputs $\bar{x}y + x\bar{y}$ and xy are sum and carry values. Outputs 0 and $x + y$ are by-products. (*b–d*) Time-lapse images of plasmodium's active zones travelling in channels of a one-bit half-adder. The dynamics of growth is shown for input values (*b*) $x = 0$ and $y = 1$, (*c*) $x = 1$ and $y = 0$, (*d*) $x = 1$ and $y = 1$. (Online version in colour.)

For input values $x = 1$ and $y = 0$, the active zones are originated at sites marked x and with an arrow in figure 9*a*. The active zone starting in the left x-input channel propagated towards the $x + y$-output of the adder. The active zone originating in the right x-input channel travelled towards $\bar{x}y + x\bar{y}$ (figure 9*c*). When both inputs are activated, $x = 1$ and $y = 1$, an active zone originated in the left y-input channel is blocked by the active zone originated in the left x-input channels. The plasmodium travelling in the right x-input channel is blocked by the active zone travelling in the right y-input channel. The active zones representing $x = 1$ and $y = 1$ enter the top-right gate P_1 and emerge at its outputs xy and $x + y$ (figure 9*d*). The Physarum adder was also implemented in chemical laboratory experiments with an excitable chemical system employing the Belousov–Zhabotinsky reaction [18].

(b) Microfluidic gates

The protoplasmic networks developed by *P. polycephalum* are living, self-growing, microfluidic systems [19–21] capable of intake and controllable delivery of biocompatible materials [22,23]. The slime mould microfluidic systems can range in size from a few millimetres to a few metres of complex protoplasmic networks with hundreds of interconnected tube fragments. To be used

Downloaded from https://royalsocietypublishing.org/ on 28 November 2024

efficiently, the protoplasmic networks must be controlled and a flow of cytoplasm transporting objects must be programmed. Vestad and co-workers [19,24] constructed logic gates by changing functional properties of a fluidic system without resorting to the nonlinear properties of a liquid. They showed that, by dynamically changing the resistance of individual channels in a microfluidic system, it is possible to direct the overall relative system of flow rates, independently of the pressure of the liquid. Their logic gates are actuated by depressing one channel of the system and reconfiguring the network [24]. Being inspired by the Vestad–Marr–Munakata results, we conducted laboratory experiments with the slime mould *P. polycephalum* and found that, when a fragment of protoplasmic tube is mechanically stimulated, a cytoplasmic flow in this fragment halts and thus resistivity increases. The cytoplasmic flow is then directed through adjacent protoplasmic tubes. We explored this phenomenon to construct several logic gates and a memory device [25].

An undisturbed Physarum exhibits more or less regular patterns of oscillations of its surface electrical potential. The electrical potential oscillations are more likely to be controlling the peristaltic activity of protoplasmic tubes, necessary for distribution of nutrients in the spatially extended body of Physarum [26,27]. A calcium ion flux through the membrane triggers oscillators responsible for controlling the dynamic of contractile activity [28,29]. The Physarum surface electrical potential oscillates with an amplitude of 1–10 mV and period 50–200 s, associated with shuttle streaming of cytoplasm [28,30–32]. Oscillations of the electrical potential and the corresponding peristaltic activity are due to calcium waves propagating along the protoplasmic tubes. These waves, and associated electrical charges and a difference in electrical potential, lead to a flow of cytoplasm.

In any given tube, cytoplasmic flow reverses its direction approximately every 54 s [25]. We can speculate that this is because calcium and peristaltic waves propagate from a root (inoculation site) of a Physarum tree towards its leaves (growth zones) and then back. That is, a protoplasmic tree is polarized and its polarization is reversed almost every minute.

When a segment of a protoplasmic tube, between two junctions, or branching points, is touched with a hair, a flow of cytoplasm inside this fragment becomes blocked. The blockage of the cytoplasmic flow could be due to K^+ channel activation, an increase in intracellular Ca^{2+}, a temporary increase in concentration of inositol trisphosphate, or activation of adenylyl cyclase; see overviews in [33,34]. A mechanically stimulated fragment restores its conductivity and the flow of cytoplasm within 54–59 s after the stimulation.

When a fragment of a tube becomes blocked, the flow of cytoplasm is directed through auxiliary, or second-order, bypassing tubes. The main, or first-order, protoplasmic tubes have a diameter *ca* 100 µm while the auxiliary, second-order, tubes have a diameter 30–40 µm. In an intact Physarum tree, the flow of cytoplasm is directed along the route with lowest resistance, i.e. along the first-order tubes, whose diameter is large. Tubes with a small diameter act as a reserve, or emergency, route for situations when large-diameter tubes are damaged or the flow is blocked. We use this phenomenon to design logic gates. A detailed example of an XOR gate is shown in figure 10 and its scheme is shown in figure 11*a–d*.

The flow is directed from '+' to '−' and then reversed from '−' to '+' (figures 10*a* and 11*a*). First-order tubes x and y represent input Boolean variables. Second-order tube z represents an output variable (figures 10*a* and 11*a*). If there is a flow of cytoplasm in a tube, the tube represents the state TRUE; if there is no flow, it is state FALSE. In an intact, or resting, state, the gate's inputs are in state '1', tubes x and y exhibit the flow of cytoplasm and tube z does not exhibit any flow: $x = 1, y = 1, z = 0$ (figures 10*b* and 11*a*). This is because tube z's diameter, *ca* 30 µm, is nearly three times smaller than the diameter of tubes x and y, *ca* 100 µm.

When tube x is touched—the moment of this mechanical stimulation is shown in figures 10*c* and 11*b*—tube x becomes 'non-conductive' and flow through tube x stops. Subsequently, the pressure in the cytoplasm increases and the cytoplasm is directed through tube z, the diameter of which increases to 70 µm due to pressure from the passing cytoplasm (figures 10*d* and 11*b*).

The gate remains in such a state for 54 s on average, and then tube x restores its conductivity. The flow of cytoplasm is then directed through tubes x and y; tube z becomes unused, shrinks due

Downloaded from https://royalsocietypublishing.org/ on 28 November 2024

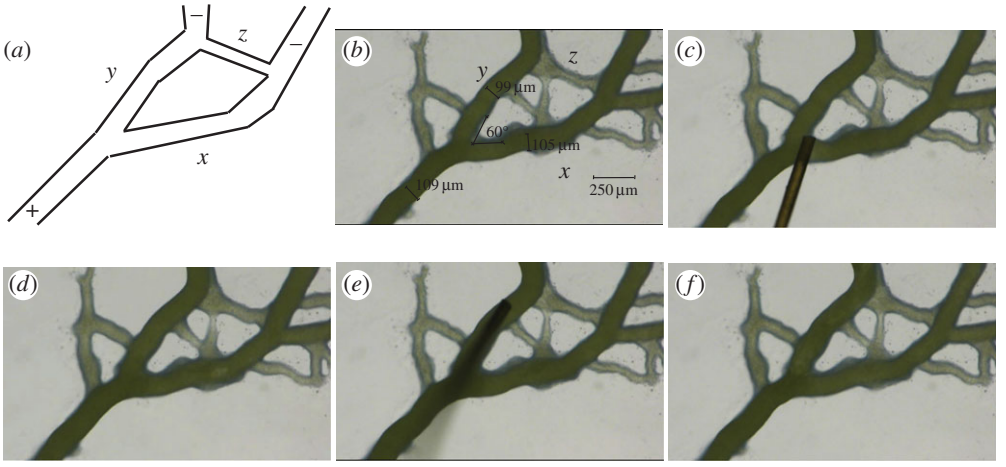

Figure 10. Implementation of an XOR gate in Physarum. (*a*) The scheme of the gate, input tubes *x* and *y* and output tube *z* are shown; '+' and '−' indicate the polarity of the cytoplasmic flow; the polarity is changing almost every minute. (*b*) Snapshot of the living gate before stimulation: $x = 1$ and $y = 1, z = 0$; some parameters of the junction are indicated. (*c*) Mechanical stimulation of tube *x*, $x = 0$. (*d*) Gate after stimulation, $x = 0, y = 1$ and $z = 1$. (*e*) Mechanical stimulation of tube *y*, $y = 0$. (*f*) Gate after stimulation, $x = 1, y = 0$ and $z = 1$. (Experimental photos courtesy of Theresa Schubert. Adapted from [25].) (Online version in colour.)

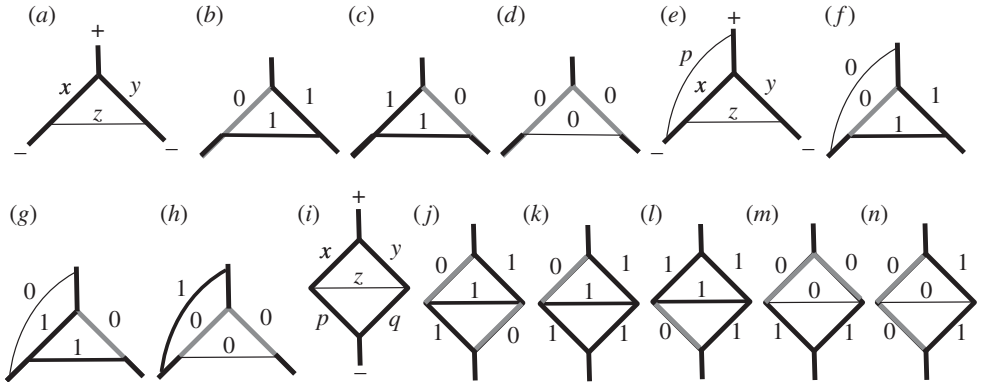

Figure 11. Schematics of gates implementable with Physarum tubes. Tubes *x* and *y* are solid black when they represent logical True, $x = 1, y = 1$, and grey when they represent logical False, $x = 0, y = 0$. Tubes *z* and *p* are thin when they represent False, $z = 0$ and $p = 0$, and they are thick when they represent True, $z = 1$ and $p = 1$. Symbols '+' and '−' indicate the polarity of the cytoplasmic flow; the polarity is changing almost every minute. (*a–d*) XOR gate, discussed in figure 10, $z = x \oplus y$, where (*a*) $x = 1, y = 1$, (*b*) $x = 0, y = 1$, (*c*) $x = 1, y = 0$, (*d*) $x = 0, y = 0$. (*e–h*) XOR and NOR gates: $z = x \oplus y$ and $p = \overline{x + y}$, where (*e*) $x = 1, y = 1$, (*f*) $x = 0, y = 1$, (*g*) $x = 1, y = 0$, (*h*) $x = 0, y = 0$. (*i–n*) Combined gate: $z = \bar{x}yp + x\bar{y}q + x\bar{p}q + yp\bar{q}$, where (*i*) $x = 1, y = 1, p = 1, q = 1$, (*j*) $x = 0, y = 1, p = 1, q = 0$, (*k*) $x = 0, y = 1, p = 1, q = 1$, (*l*) $x = 1, y = 1, p = 0, q = 1$, (*m*) $x = 0, y = 0, p = 1, q = 1$, (*n*) $x = 0, y = 1, p = 0, q = 1$. (Adapted from [25].)

to elasticity and its diameter returns to a resting value of 30 µm. This is somewhat analogous to an automated adjustment employed for microfluidic implementations of a Wheatstone bridge [35]. The state of the gate after mechanical stimulation of tube *y* (figure 10*e*) is shown in figures 10*f* and 11*c*. The gate restores its original state in less than a minute after mechanical stimulation. When a flow stops in *x* and *y* at the same time, the flow may not occur in tube *z* because the tube becomes isolated from the upper part of the protoplasmic network. Therefore, we assume that $z = 0$ if $x = 0$ and $y = 0$. Thus, the XOR gate is implemented, $z = x \oplus y$ (figure 11*a–d*).

Downloaded from https://royalsocietypublishing.org/ on 28 November 2024

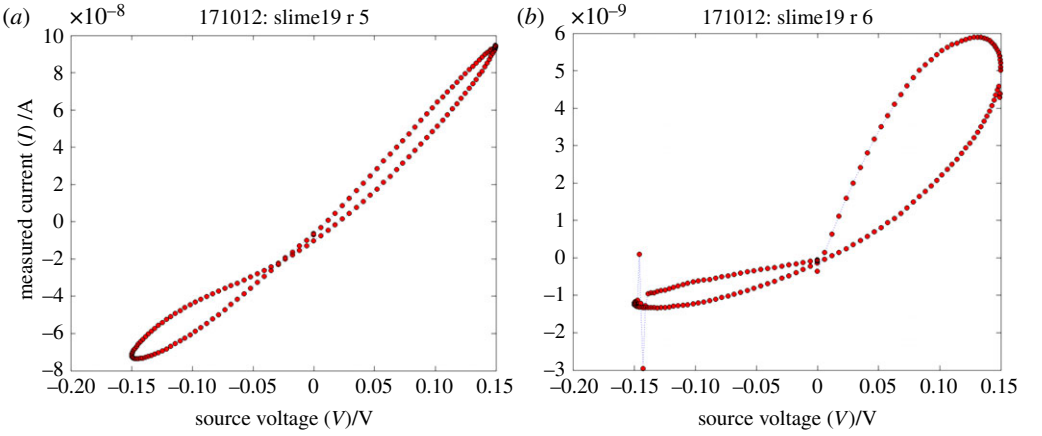

Figure 12. Typical current versus voltage profiles recorded in laboratory experiments with slime mould *P. polycephalum*. (Courtesy of Ella Gale. Adapted from [39].) (Online version in colour.)

By adding one more second-order tube to gate XOR (figure 11*a–d*), we produce a gate with two inputs and two outputs (figure 11*e–h*). The gate is shown in figure 11*e–h*. It computes exclusive disjunction and negated disjunction in parallel. The output tube $z = x \oplus y$ acts in a manner similar to the XOR gate (figure 11*a–d*). The output tube $p = \overline{x + y}$ connects the inlet of tube x, just before the junction of x and z, to the outlet of the junction of the tubes x and y. Cytoplasmic flow is directed via tube p; $p = 1$ only if tubes x and y are blocked, $x = 0$ and $y = 0$ (figure 11*h*).

By adding two more first-order tubes to gate XOR (figure 11*a–d*), we produce a gate with four inputs and one output (figure 11*i–n*). The gate $z = \bar{x}yp + x\bar{y}q + x\bar{p}q + yp\bar{q}$ (figure 11*i–n*) responds with value TRUE only when one input tube is blocked yet two of its neighbouring input tubes are unblocked. Examples are as follows. Tubes x and q are blocked, $x = 0$ and $q = 0$, tubes y and p are unblocked, $y = 1$ and $p = 1$ (figure 11*j*), flow is directed via tube z. Tubes y, p, q are unblocked, $y = 1$, $p = 1$, $q = 1$, tube x is blocked, $x = 0$ (figure 11*k*), flow is directed via tube z. Tubes x, y and q are unblocked and tube p is blocked (figure 11*l*), flow is directed via tube z. For all other combinations of input tuples, the output is FALSE. Examples are as follows. Tubes x and y are blocked and tubes p and q are unblocked (figure 11*m*), there is no flow of cytoplasm through the gate and thus $z = 0$. Tubes x and p are blocked and tubes y and q are unblocked (figure 11*n*), cytoplasm is flowing through tubes y and q and thus $z = 0$.

4. Memristor

A memristor is a resistor with a memory, the resistance of which depends on how much current has flowed through the device. Memristors [36] have revolutionized the material basis of computation [37,38]. A memristor is a material implication $\rightarrow$, a universal Boolean logic gate. For example, $\overline{xy} = x \rightarrow (y \rightarrow 0)$ or $x + y = (x \rightarrow 0) \rightarrow y$ or $x \oplus y = (x \rightarrow y) \rightarrow ((y \rightarrow x) \rightarrow 0)$.

In laboratory experiments [39], we demonstrated that protoplasmic tubes of acellular slime mould *P. polycephalum* show current versus voltage profiles consistent with memristive systems (figure 12). Experimental laboratory studies show pronounced hysteresis and memristive effects exhibited by the slime mould. Being a memristive element, the slime mould's protoplasmic tube can also act as a low-level sequential logic element [40] operated with current spikes, or current transients. In such a device, logical input bits are temporarily separated.

The memristive properties of the slime mould's protoplasmic tubes gives us a hope that a range of 'classical' memristor-based neuromorphic architectures [41–46] can be implemented with *P. polycephalum*. A memristor is an analogue of a synaptic connection [43,47]: the memristor is

Downloaded from https://royalsocietypublishing.org/ on 28 November 2024

capable of direct emulation of the temporal dynamics of real-life synapses [48]. Being a living memristor, each protoplasmic tube of Physarum is a synaptic element with memory, the state of which is modified depending on its pre-synaptic and post-synaptic activities. By analogy with memristors, several protoplasmic tubes in a Physarum network can form an associative memory network [43].

5. Sensors

The slime mould never rests. It shifts its cytoplasm periodically between distant parts of its body. The cytoplasm is moved by peristaltic contractions of the slime mould's protoplasmic tubes. The peristaltic movement is associated with propagation of calcium waves and oscillations of surface electrical potential. The Physarum responds to external stimulation by changing the frequency and amplitude of the electrical potential oscillation. We show how to map mechanical (§5a), chemical (§5b) and optical (§5c) stimuli to patterns of the electrical potential oscillations and thus design a range of hybrid sensors from the slime mould.

A typical experimental design of a Physarum sensor is shown in figure 13. Each electrode is made of a conductive aluminium foil, 0.07 mm thick, 8 mm wide, 50 mm (including the part protruding outside the Petri dish) long. Two blobs of agar (2 ml each; figure 13*b*) were placed on the electrodes (figure 13*c*) stuck to the bottom of a plastic Petri dish (9 cm). The distance between the proximal sites of the electrodes is always 10 mm. The Physarum was inoculated on one agar blob. We waited until the Physarum colonized the first blob, where it was inoculated, and propagated towards and colonized the second blob. When the second blob was colonized, the two blobs of agar, both colonized by Physarum (figure 13*a*), became connected by a single protoplasmic tube (figure 13*d*).

(a) Tactile sensor

Physarum exhibits more or less classical oscillations before stimulation (figure 14*a*), but the shape of the oscillatory waves is a bit distorted, possibly due to minor branches of the tube connecting the blobs and electrodes. When a segment of a glass capillary tube is placed across a protoplasmic tube, the Physarum demonstrates two types of response to application of this load: an immediate response with a high-amplitude impulse (figure 14*b*) and a prolonged response with changes in the oscillation pattern (figure 14*c*) [49]. The immediate response is a high-amplitude spike: its amplitude is 12.33 mV and its duration is 150 s. The prolonged response is an envelope of increased amplitude oscillations. The average amplitude of oscillations before stimulation, in the example shown in figure 14, was 2.3 mV and the duration of each wave was 120 s. The amplitude of the waves in the prolonged response became 5.29 mV, with the duration of a wave slightly increased to 124 s.

The slime mould of *P. polycephalum* reacts to the application and removal of a load with a high-amplitude impulse and with a temporary change of its oscillatory activity pattern [49]. There are two possible types of response: an immediate response in the form of a high-amplitude impulse and a prolonged response in the form of changes in oscillation frequency and amplitude.

Most animals also have receptors in hair follicles, including hairs in the skin and hair cells in the cochlea. The receptive terminals typically react to their stretching when a hair is deflected. To make tactile hair with Physarum, we used the set-up shown in figure 13 but with a hair rooted in the agar blob on the recording electrode [50]. Typically, 1–3 days after inoculation of Physarum to an agar blob on a reference electrode, it propagates to and colonizes the agar blob on a recording electrode. A slime mould analogue of a neuron terminal connecting two blobs of Physarum is formed. Physarum 'climbs' onto the hair and occupies one-third to one-half of the hair length (figure 15*a*). In many cases, a sub-network of protoplasmic tubes is formed around the base of the hair.

A typical response of Physarum to stimulation is shown in figure 15*b*. The response comprises an immediate response—a high-amplitude impulse—and a prolonged response. The

Downloaded from https://royalsocietypublishing.org/ on 28 November 2024

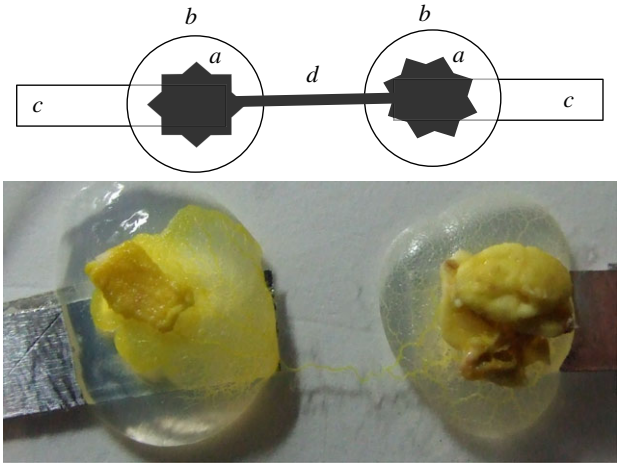

Figure 13. Typical configuration of a Physarum sensor. (Top) The experimental set-up: (*a*) Physarum, (*b*) agar blobs, (*c*) electrodes, (*d*) protoplasmic tube. All parts of Physarum shown in dark grey form a single cell. (Bottom) A protoplasmic tube connects two blobs of agar lying on electrodes. (Online version in colour.)

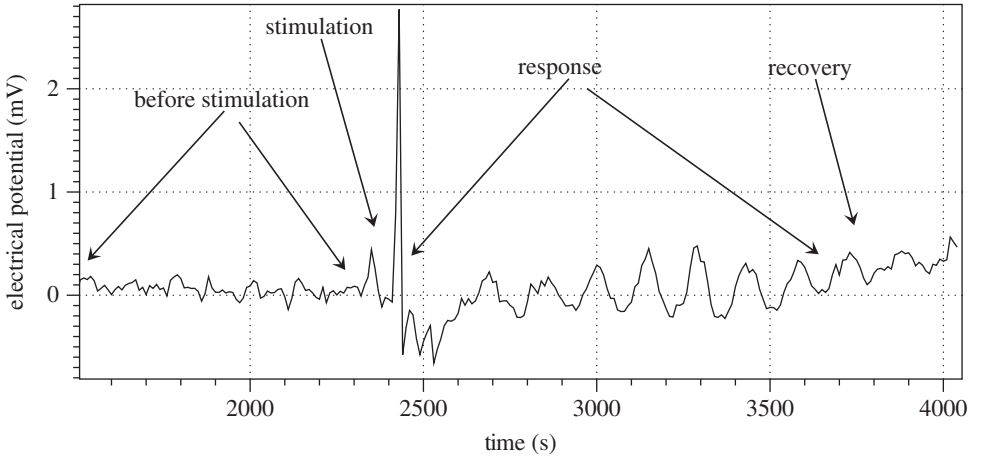

Figure 14. Physarum's response to application of a 0.05 g load. The *y*-axis shows the electrical potential value in mV, whereas the *x*-axis shows the time in seconds. A glass capillary tube weighing 0.05 g is applied across the protoplasmic tube at 2400 s from the beginning of recording. We can observe the following patterns: oscillation before stimulation, immediate response to stimulation, prolonged response to stimulation, return to normal oscillatory activity. (See details in [49].)

high-amplitude impulse is always well pronounced, but prolonged response oscillations can sometimes be distorted by other factors, e.g. growing branches of a protoplasmic tube or additional strands of plasmodium propagating between the agar blobs. Responses are repeatable not only in different experiments but also during several rounds of stimulation in the same experiment [50].

(b) Chemical sensor

Slime mould *P. polycephalum* is sensitive to volatile aromatic substances [12,51]. The experiments described in [12,51] laid the foundation for the laboratory prototyping of a Physarum-based chemical sensor [52]. Based on previous extensive testing of Physarum binary preferences

Downloaded from https://royalsocietypublishing.org/ on 28 November 2024

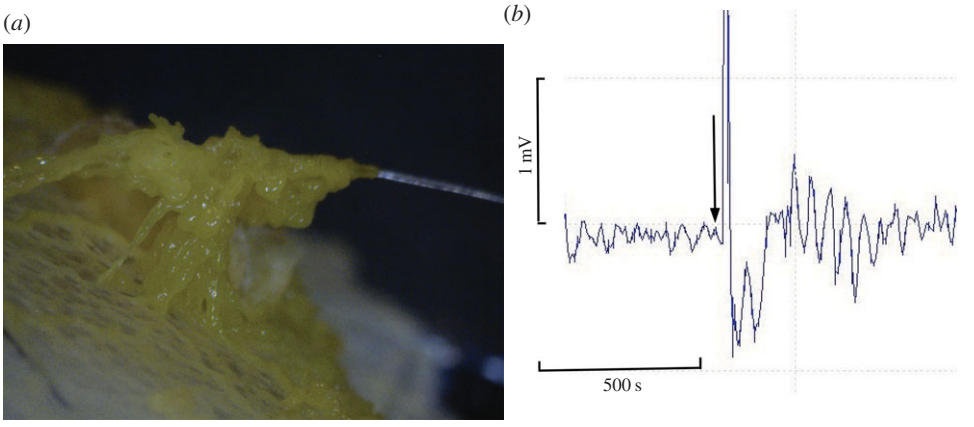

Figure 15. Slime mould tactile hair. (*a*) Photograph of the experimental set-up: a hair is partly colonized by slime mould. (*b*) Typical responses of Physarum to deflection of the hair. The *y*-axis is the electrical potential value in mV, whereas the *x*-axis is the time in seconds. Physarum responds with a high-amplitude impulse and an envelope of four or five waves. The moment of hair deflection is shown by the arrow. (See details in [50].) (Online version in colour.)

to various volatile chemicals [53], Whiting *et al.* [52] derived an experimental mapping between subsets of chemoattractants and chemorepellents: farnesene, tridecane, s(–)limonene, cis-3-hexenylacetate, geraniol, benzyl alcohol, linalool and nonanal (figure 16). The slime mould's reaction to the strongest—as demonstrated in binary choice experiments [53]—attractants (farnesene, tridecane, s(–)limonene, cis-3-hexenylacetate) is manifested by the increase in the frequency of the electrical potential oscillations. Repellents (linalool, benzyl alcohol, nonanal) were indicated by a decrease in oscillation frequency, and, in the case of linlool and benzyl alcohol, a substantial increase in the oscillation amplitude. Thus, Whiting *et al.* [52] have shown that *P. polycephalum* can identify individual chemicals by the relative amplitude and frequency change after exposure; the detection of chemicals can occur at 4 cm, without diffusion through a growth medium such as agar. It is possible that this set-up could be employed as a chemical sensor, allowing the contactless detection of volatile organic components as well as potentially other chemicals.

(c) Colour sensor

The plasmodium of *P. polycephalum* shows a substantial degree of photo-sensitivity. A plasmodium moves away from light when it can or switches to another phase of its life cycle or undergoes fragmentation when it cannot escape from light. If a plasmodium, especially a starving one [54], is subjected to a high intensity of light, the plasmodium turns into a sporulation phase [55]. The illumination increase causes changes in the plasmodium's oscillatory activity; the degree of change is proportional to the distance from the light source [56,57].

In laboratory experiments, described in detail in [58], we studied the Physarum reaction to light of different colours. The Physarum, which was based on a recording electrode, was illuminated from above using a white LED (1400 LUX) with a set of colour lenses: red (635 nm), green (560 nm) and blue (450 nm). We also illuminated Physarum with white light via a transparent lens. The amount of light on the blob was 80–120 LUX for each colour. In each experiment, we recorded the electrical activity of Physarum in darkness (10 min), under illumination (10 min) and after illumination was removed (10 min) (figure 17).

We found that the slime mould recognizes a colour because it reacts to illumination with the colour by unique changes in amplitude and periods of oscillatory activity. We found that Physarum recognizes when red and blue light are switched ON and when red light is switched

Downloaded from https://royalsocietypublishing.org/ on 28 November 2024

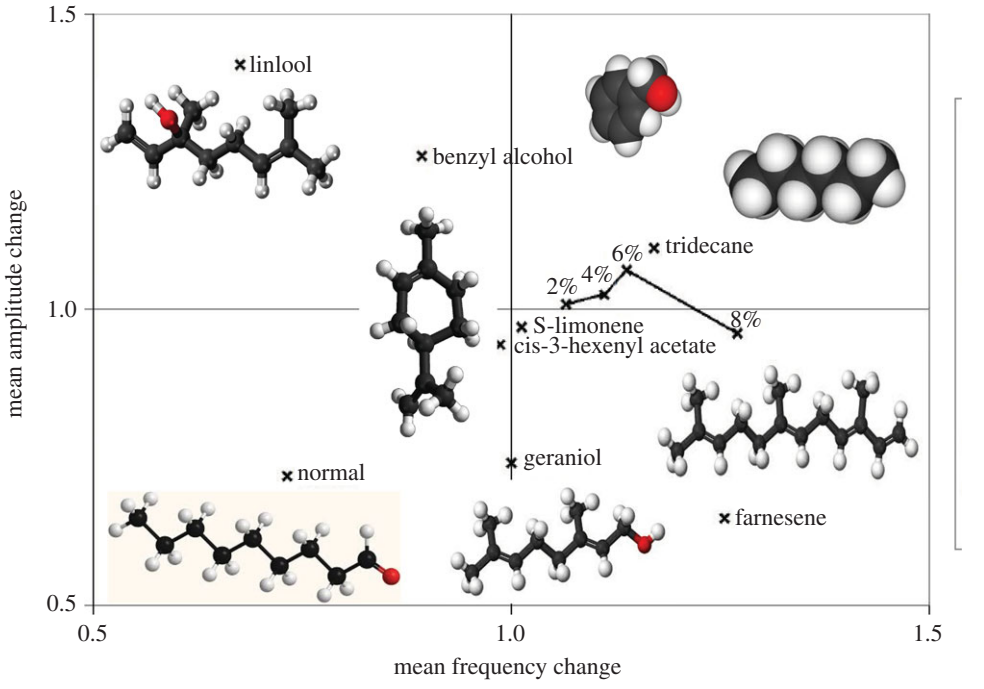

Figure 16. The Physarum chemical sensor reacts by changes in the amplitude and frequency of oscillations to exposure to volatile chemicals. (Adapted from [52].) (Online version in colour.)

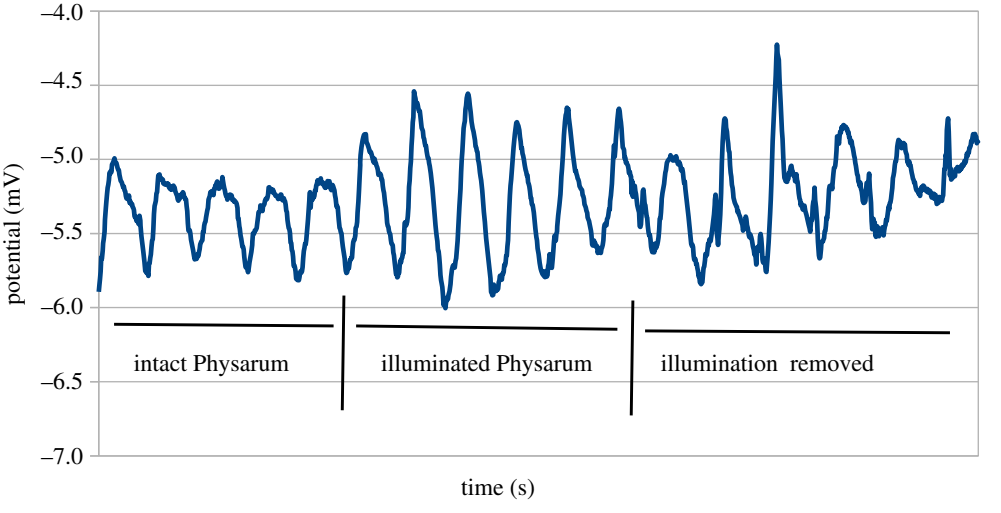

Figure 17. Patterns of oscillations of Physarum surface electrical potential before, during and after illumination with blue light. (See details in [58].) (Online version in colour.)

OFF [58]. Red and blue illuminations decrease the frequency of oscillations, i.e. increase the period. Red light increases the amplitude of oscillations but blue light decreases the amplitude. Physarum does not differentiate between green and white lights. Switching off all lights but red leads to a decrease in both the amplitude and frequency of oscillations. Switching off the red light leads to an increase of periods and decrease of amplitudes of oscillations.

Downloaded from https://royalsocietypublishing.org/ on 28 November 2024

The diversity of oscillations, calculated as the standard deviation of amplitudes or periods, is another useful characteristic of the Physarum response to illumination. In terms of the diversity of oscillations, Physarum recognizes when white and green colours are switched on. Also in terms of the diversity of oscillations, Physarum recognizes that illumination is switched off (its oscillating behaviour becomes uniform) but does not recognize which exact colour is switched off. Switching off all types of illumination decreases the diversity of amplitudes and periods.

The increase in diversity of oscillations might be explained by the formation of additional micro-oscillators in the Physarum protoplasmic networks. The phases and frequencies of the oscillations and the positions of the micro-oscillators relative to each other lead to the emergence of waveforms with different amplitudes and periods, as recorded in experiments. Switching off illumination may extinguish some of the micro-oscillators, so that Physarum reacts to switching off the illumination by producing rather uniform patterns of oscillation [58].

6. Conclusion

We have demonstrated the polymorphism of the computing potential of slime mould on a series of problems from computational geometry, path finding and implementation of logic gates. We have also shown how inputs can be fed into the slime mould circuits using mechanical, chemical and optical stimuli. The slime mould *P. polycephalum* computes by leaving uninhabited loci of substrate (Voronoi diagram), by encapsulating datasets with its protoplasmic tubes (α-shapes), by following gradients of chemoattractants (maze), by competing between active growing zones (ballistic logic gates), but halting and rerouting its cytoplasmic streams (microfluidic logic gates), and by changing patterns of its electrical potential oscillations (sensors).

Which of these prototypes exemplifies heterotic computers? Each of them.

When constructing the Voronoi diagram, Physarum expands as a unidirectional wave from each site of inoculation. No attractants are involved. Thus, we could assume that the computation is performed exclusively by the slime mould placed in an 'empty space'. This is not exactly true: the slime mould propagates as an omnidirectional wave only on the nutrient-rich substrate. Physarum grows as a tree on a non-nutrient substrate, thus making construction of a Voronoi diagram impossible. That is, the substrate assists the slime mould to do computation.

Ballistic slime mould gates also do not require any additional stimulation (albeit they work better with one) because of the 'inertial' movement of the slime mould. However, propagation of the slime mould's active growing zones is constrained by the geometry of the agar gate. Physarum and the mechanical substrate do computation together. Slime mould processors computing a convex hull and maze are definitely heterotic: the slime mould is attracted by nutrients towards data points in the convex hull and targets in the maze. Microfluidic logic gates and sensors require mechanical, chemical and optical inputs to process information.

When I was giving my talk on the slime mould computing and presented maze-solving, Professor Susan Stepney asked me 'What is the computing entity: Physarum propagating in the maze towards the target or chemicals diffusing from the target source of nutrients?' The answer is 'neither' and 'both'. Chemicals *per se* do not compute, they only diffuse. The slime mould *per se* does not compute—it simply follows gradients of diffusing chemicals. When combined together as an indistinguishable device, they perform computation. This is the power of heterotic computing.

Funding statement. This work is part of the Physarum Chip project funded by the Seventh Framework Programme (FP7) of the European Commission within CORDIS and the FET Proactive scheme.

References

1. Stephenson SL, Stempen H. 2000 *Myxomycetes: a handbook of slime molds*. Portland, OR: Timber Press.
2. Nakagaki T, Yamada H, Toth A. 2000 Maze-solving by an amoeboid organism. *Nature* **407**, 470–470. (doi:10.1038/35035159)

Downloaded from https://royalsocietypublishing.org/ on 28 November 2024

3. Nakagaki T, Yamada H, Toth A. 2001 Path finding by tube morphogenesis in an amoeboid organism. *Biophys. Chem.* **92**, 47–52. (doi:10.1016/S0301-4622(01)00179-X)
4. Nakagaki T, Iima M, Ueda T, Nishiura Y, Saigusa T, Tero A, Kobayashi R, Showalter K. 2007 Minimum-risk path finding by an adaptive amoeba network. *Phys. Rev. Lett.* **99**, 068104. (doi:10.1103/PhysRevLett.99.068104)
5. Adamatzky A. 2010 *Physarum machines: making computers from slime mould*. Singapore: World Scientific.
6. Preparata FP, Shamos MI. 1985 *Computational geometry: an introduction*. New York, NY: Springer.
7. Adamatzky A, De Lacy Costello B, Asai T. 2005 *Reaction–diffusion computers*. Amsterdam, The Netherlands: Elsevier.
8. Edelsbrunner H, Kirkpatrick D, Seidel R. 1983 On the shape of a set of points in the plane. *IEEE Trans. Inform. Theor.* **29**, 551–559. (doi:10.1109/TIT.1983.1056714)
9. Edelsbrunner H, Muke EP. 1994 Three-dimensional alpha shapes. *ACM Trans. Graph.* **13**, 43–72. (doi:10.1145/174462.156635)
10. Jarvis R. 1973 On the identification of the convex hull of a finite set of points in the plane. *Inform. Process. Lett.* **2**, 18–21. (doi:10.1016/0020-0190(73)90020-3)
11. Adamatzky A. 2012 Slime mould computes planar shapes. *Int. J. Bio-Inspired Comput.* **4**, 149–154. (doi:10.1504/IJBIC.2012.047239)
12. Adamatzky A. 2012 Simulating strange attraction of acellular slime mould *Physarum polycephalum* to herbal tablets. *Math. Comput. Model.* **55**, 884–900. (doi:10.1016/j.mcm.2011.09.015)
13. Shannon C. 1951 Presentation of a maze solving machine. In *Trans. 8th Conf. Cybernetics: Circular, Causal and Feedback Mechanisms in Biological and Social Systems*, *New York, NY, 15–16 March 1951*, pp. 169–181. New York, NY: Josiah Macy, Jr. Foundation.
14. Reyes DR, Ghanem MM, Whitesides GM, Manz A. 2002 Glow discharge in microfluidic chips for visible analog computing. *Lab Chip* **2**, 113–116. (doi:10.1039/b200589a)
15. Lagzi I, Soh S, Wesson PJ, Browne KP, Grzybowski BA. 2010 Maze solving by chemotactic droplets. *J. Am. Chem. Soc.* **132**, 1198–1199. (doi:10.1021/ja9076793)
16. Adamatzky A. 2009 Hot ice computer. *Phys. Lett. A* **374**, 264–271. (doi:10.1016/j.physleta.2009.10.072)
17. Adamatzky A. 2009 Slime mould logical gates. (http://arxiv.org/abs/1005.2301v1)
18. De Lacy Costello B, Adamatzky A, Jahan I, Zhang L. 2011 Towards constructing one-bit binary adder in excitable chemical medium. *Chem. Phys.* **381**, 88–99. (doi:10.1016/j.chemphys.2011.01.014)
19. Marr DWM, Munakata T. 2007 Micro/nanofluidive computing. *Commun. ACM* **50**, 64–68. (doi:10.1145/1284621.1284650)
20. Kirby B. 2010 *Micro- and nanoscale fluid mechanics: transport in microfluidic devices*. Cambridge, UK: Cambridge University Press.
21. Tabeling P. 2010 *Introduction to microfluidics*. Oxford, UK: Oxford University Press.
22. Adamatzky A. 2010 Manipulating substances with *Physarum polycephalum*. *Mater. Sci. Eng. C* **30**, 1211–1220. (doi:10.1016/j.msec.2010.06.020)
23. Mayne R, Patton D, De Lacy Costello B, Adamatzky A, Patton RC. 2014 On the internalisation, intraplasmodial carriage and excretion of metallic nanoparticles in the slime mould, *Physarum polycephalum*. *Int. J. Nanotechnol. Mol. Comput.* **3**, 1–14. (doi:10.4018/ijnmc.2011070101)
24. Vestad T, Marr DWM, Munakata T. 2004 Flow resistance for microfluidic logic operations. *Appl. Phys. Lett.* **84**, 5074–5075. (doi:10.1063/1.1764592)
25. Adamatzky A, Schubert T. 2014 Slime mould microfluidic logical gates. *Mater. Today* **17**, 86–91. (doi:10.1016/j.mattod.2014.01.018)
26. Seifriz W. 1937 A theory of protoplasmic streaming. *Science* **86**, 397–402. (doi:10.1126/science.86.2235.397)
27. Heilbrunn LV, Daugherty K. 1939 The electric charge of protoplasmic colloids. *Physiol. Zool.* **12**, 1–12.
28. Meyer R, Stockem W. 1979 Studies on microplasmodia of *Physarum polycephalum* V: electrical activity of different types of micro- and macroplasmodia. *Cell Biol. Int. Rep.* **3**, 321–330. (doi:10.1016/S0309-1651(79)80002-8)
29. Fingerle J, Gradmann D. 1982 Electrical properties of the plasma membrane of microplasmodia of *Physarum polycephalum*. *J. Memb. Biol.* **68**, 67–77. (doi:10.1007/BF01872255)

Downloaded from https://royalsocietypublishing.org/ on 28 November 2024

30. Iwamura T. 1949 Correlations between protoplasmic streaming and bioelectric potential of a slime mould, *Physarum polycephalum*. *Bot. Mag.* **62**, 126–131. (doi:10.15281/jplantres1887.62.126)
31. Kamiya N, Abe S. 1950 Bioelectric phenomena in the myxomycete plasmodium and their relation to protoplasmic flow. *J. Colloid. Sci.* **5**, 149–163. (doi:10.1016/0095-8522(50)90016-X)
32. Kashimoto U. 1958 Rhythmicity on the protoplasmic streaming of a slime mold, *Physarum Polycephalum*. I. A statistical analysis of the electric potential rhythm. *J. Gen. Physiol.* **41**, 1205–1222. (doi:10.1085/jgp.41.6.1205)
33. Hamil OP, Martinac B. 2001 Molecular basis of mechanotransduction in living cells. *Physiol. Rev.* **81**, 685–740.
34. Kamm RD, Kaazempur-Mofrad MR. 2004 On the molecular basis for mechanotransduction. *Mech. Chem. Biosyst.* **1**, 201–209.
35. Tanyeri M, Ranka M, Sittipolkula N, Schroeder CM. 2011 Microfluidic Wheatstone bridge for rapid sample analysis. *Lab Chip* **11**, 4181–4186. (doi:10.1039/c1lc20604d)
36. Chua L. 1971 Memristor — the missing circuit element. *IEEE Trans. Circuit Theory* **18**, 507–519. (doi:10.1109/TCT.1971.1083337)
37. Strukov DB, Sinder GS, Williams RS. 2008 The missing memristor found. *Nature* **453**, 80–83. (doi:10.1038/nature06932)
38. Williams RS. 2013 Aftermath of finding the memristor. In *Chaos, CNN, memristors and beyond* (eds A Adamatzky, R Chen), pp. 490–493. Singapore: World Scientific.
39. Gale E, De Lacy Costello B, Adamatzky A. 2013 Slime mould memristors. (http://arxiv.org/abs/1306.3414)
40. Gale E, De Lacy Costello B, Adamatzky A. 2013 Boolean logic gates from a single memristor via low-level sequential logic. In *Unconventional computation and natural computation* (eds G Mauri, A Dennunzio, L Manzoni, AE Porreca), pp. 79–89. Lecture Notes in Computer Science, vol. 7956. Berlin, Germany: Springer.
41. Smerieri A, Berzina T, Erokhin V, Fontana MP. 2008 Polymeric electrochemical element for adaptive networks: pulse mode. *J. Appl. Phys.* **104**, 114 513–114 513. (doi:10.1063/1.3033399)
42. Jo SH, Chang T, Ebon I, Bhadviya BB, Mazumder P, Lu W. 2010 Nanoscale memristor devices as a synapse in neuromorphic systems. *Nano. Lett.* **10**, 1297–1301. (doi:10.1021/nl904092h)
43. Pershin YV, Di Ventra M. 2010 Experimental demonstration of associative memory with memristive neural networks. *Neural Netw.* **23**, 881–886. (doi:10.1016/j.neunet.2010.05.001)
44. Howard G, Gale E, Bull L, de Lacy Costello B, Adamatzky A. 2012 Evolution of plastic learning in spiking networks via memristive connections. *IEEE Trans. Evol. Comput.* **16**, 711–729. (doi:10.1109/TEVC.2011.2170199)
45. Erokhin V, Howard GD, Adamatzky A. 2012 Organic memristor devices for logic elements with memory. *Int. J. Bifurcation Chaos* **22**, 1250283. (doi:10.1142/S0218127412502835)
46. Gale E, de Lacy Costello B, Adamatzky A. 2013 Observation, characterization and modeling of memristor current spikes. *Appl. Math. Inform. Sci.* **7**, 1395–1403. (doi:10.12785/amis/070418)
47. Cai W, Tetzlaff R, Ellinger F 2011 A memristive model compatible with triplet rule for spike-timing-dependent-plasticity. (http://arxiv.org/abs/1108.4299)
48. Indiveri G, Linares-Barranco B, Legenstein R, Deligeorgis G, Prodromakis T. 2013 Integration of nanoscale memristor synapses in neuromorphic computing architectures. *Nanotechnology* **24**, 384010. (doi:10.1088/0957-4484/24/38/384010)
49. Adamatzky A. 2013 Slime mould tactile sensor. *Sens. Actuators B Chem.* **188**, 38–44. (doi:10.1016/j.snb.2013.06.050)
50. Adamatzky A. 2014 Tactile bristle sensors made with slime mould. *Sens. J. IEEE* **14**, 324–332. (doi:10.1109/JSEN.2013.2283192)
51. Adamatzky A. 2011 On attraction of slime mould *Physarum polycephalum* to plants with sedative properties. *Nature Precedings*. (doi:10.1038/npre.2011.5985.1)
52. Whiting JGH, de Lacy Costello BPJ, Adamatzky A. 2011 Towards slime mould chemical sensor: mapping chemical inputs onto electrical potential dynamics of *Physarum polycephalum*. *Sens. Actuators B Chem.* **19**, 844–853.
53. De Lacy Costello B, Adamatzky A. 2013 Assessing the chemotaxis behavior of *Physarum polycephalum* to a range of simple volatile organic chemicals. *Commun. Integr. Biol.* **6:5**, e25030.
54. Guttes E, Guttes S, Rusch HP. 1961 Morphological observations on growth and differentiation of *Physarum polycephalum* grown in pure culture. *Dev. Biol.* **3**, 588–614. (doi:10.1016/0012-1606(61)90034-3)

55. Sauer HW, Babcock KL, Rusch HP. 1969 Sporulation in *Physarum polycephalum*: a model system for studies on differentiation. *Exp. Cell Res.* **57**, 319–327. (doi:10.1016/0014-4827(69)90156-6)
56. Wohlfarth-Bottermann KE, Block I. 1981 The pathway of photosensory transduction in *Physarum polycephalum*. *Cell Biol. Int. Rep.* **5**, 365–373. (doi:10.1016/0309-1651(81)90006-0)
57. Block I, Wohlfarth-Bottermann KE. 1981 Blue light as a medium to influence oscillatory contraction frequency in *Physarum*. *Cell Biol. Int. Rep.* **5**, 73–81. (doi:10.1016/0309-1651(81)90160-0)
58. Adamatzky A. 2013 Towards slime mould colour sensor: recognition of colours by *Physarum polycephalum*. *Organ. Electron.* **14**, 3355–3361. (doi:10.1016/j.orgel.2013.10.004)

Downloaded from https://royalsocietypublishing.org/ on 28 November 2024